Altered fatty acid metabolism rewires cholangiocarcinoma stemness features

Giulia Lori, Mirella Pastore, Nadia Navari, Benedetta Piombanti, Richell Booijink, Elisabetta Rovida, Ignazia Tusa, Monika Lewinska, Jesper B. Andersen, Tiziano Lottini, Annarosa Arcangeli, Maria Letizia Taddei, Erica Pranzini, Caterina Mancini, Cecilia Anceschi, Stefania Madiai, Elena Sacco, Stefano Rota, Adriana Trapani, Gennaro Agrimi, Matteo Ramazzotti, Paola Ostano, Caterina Peraldo Neia, Matteo Parri, Fabrizia Carli, Silvia Sabatini, Amalia Gastaldelli, Fabio Marra, Chiara Raggi

PII: S2589-5559(24)00186-1

DOI: https://doi.org/10.1016/j.jhepr.2024.101182

Reference: JHEPR 101182

To appear in: *JHEP Reports*

Received Date: 5 August 2023

Revised Date: 26 July 2024

Accepted Date: 30 July 2024

Please cite this article as: Lori G, Pastore M, Navari N, Piombanti B, Booijink R, Rovida E, Tusa I, Lewinska M, Andersen JB, Lottini T, Arcangeli A, Taddei ML, Pranzini E, Mancini C, Anceschi C, Madiai S, Sacco E, Rota S, Trapani A, Agrimi G, Ramazzotti M, Ostano P, Neia CP, Parri M, Carli F, Sabatini S, Gastaldelli A, Marra F, Raggi C, Altered fatty acid metabolism rewires cholangiocarcinoma stemness features, *JHEP Reports*, https://doi.org/10.1016/j.jhepr.2024.101182.

iCCA-2D

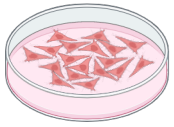

Fatty acids

iCCA-3D

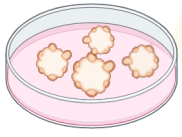

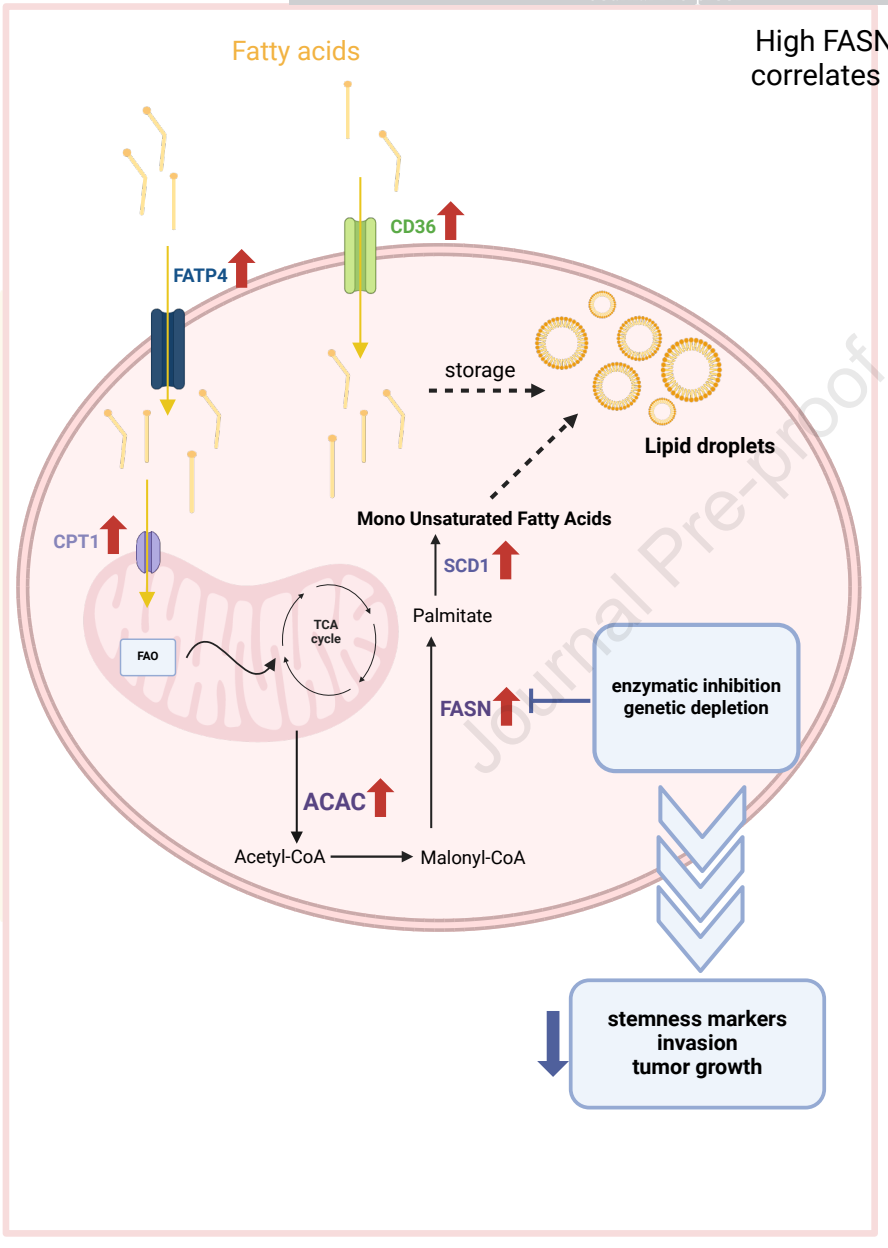

High FASN level correlates with:

iCCA patients (n=68)

Worst prognosis

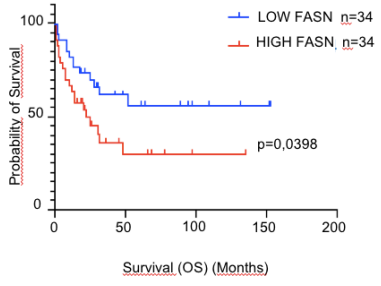

Adverse prognostic factors

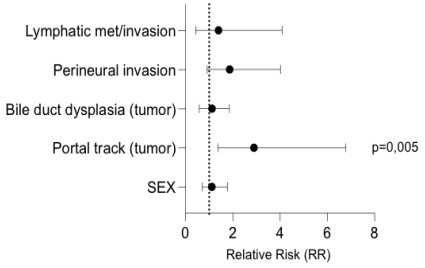

Expression of stem-related genes

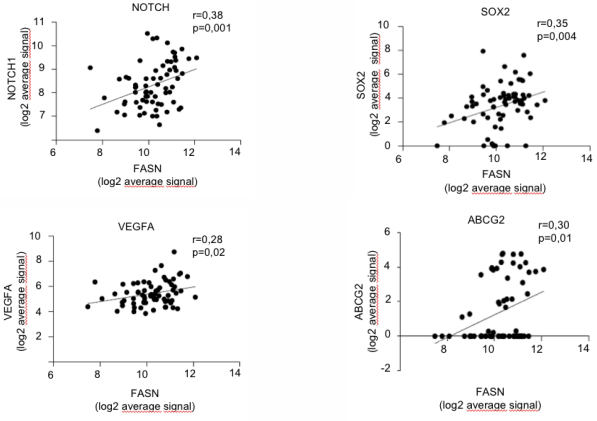

Altered fatty acid metabolism rewires cholangiocarcinoma stemness features

Giulia Lori[1], Mirella Pastore[1], Nadia Navari[1], Benedetta Piombanti[1], Richell Booijink[2], Elisabetta Rovida[3], Ignazia Tusa[3], Monika Lewinska[4], Jesper B. Andersen[4], Tiziano Lottini[1], Annarosa Arcangeli[1], Maria Letizia Taddei[1], Erica Pranzini[3], Caterina Mancini[1], Cecilia Anceschi[3], Stefania Madiai[1], Elena Sacco[5], Stefano Rota[5], Adriana Trapani[6], Gennaro Agrimi[7], Matteo Ramazzotti[3], Paola Ostano[8], Caterina Peraldo Neia[8], Matteo Parri[3], Fabrizia Carli[9], Silvia Sabatini[9], Amalia Gastaldelli[9], Fabio Marra[1*#] and Chiara Raggi[1*#].

*Co-seniorship

Corresponding Author

[1] Department of Experimental and Clinical Medicine, University of Florence, Florence, Italy;
[2] Department of Biomaterial Science and Technology, University of Twente Enschede, The Netherlands;
[3] Department of Experimental and Clinical Biomedical Sciences, University of Florence, Florence, Italy;
[4] Biotech Research and Innovation Centre, Department of Health and Medical Sciences, University of Copenhagen, Copenhagen, Denmark;
[5] Department of Biotechnology and Biosciences, University of Milano-Bicocca, Milan, Italy;
[6] Department of Pharmacy-Drug Sciences, University of Bari, Bari, Italy;
[7] Department of Biosciences, Biotechnologies and Environment, University of Bari, Bari, Italy;
[8] Cancer Genomics Lab, Fondazione Edo ed Elvo Tempia, Biella, Italy;
[9] Institute of Clinical Physiology, National Research Council, CNR, Pisa, Italy.

Contact:
Chiara Raggi, PhD
Department of Experimental and Clinical Medicine, University of Florence
Cubo Centro Polivalente 2
Viale Pieraccini, 6
I50134 Florence, Italy
Email: chiara.raggi@unifi.it
Phone+390552758128

and / or

Fabio Marra, MD, PhD
Department of Experimental and Clinical Medicine, University of Florence
Largo Brambilla, 3
I50134 Florence, Italy
Email: fabio.marra@unifi.it
Phone+390557945425

Key Words: hepatobiliary tumors, cancer stem cells, lipid metabolism, oleic acid, palmitoleic acid, triglycerides, lipid droplets

List of Abbreviations: iCCA, intrahepatic cholangiocarcinoma; CSCs, cancer stem cells, EMT, epithelial to mesenchymal transition; FAs, fatty acids; FASN, Fatty Acid Synthase; AceCS1, cytoplasmic acetyl-CoA synthetase; ACLY, ATP citrate lyase; ACAC, Acetyl-CoA carboxylase; ACSL1, Acyl-CoA Synthetase Long Chain Family Member 1; GSEA, gene set-enrichment analysis; MON, monolayer; OA, Oleic Acid; POA, Palmitoleic Acid; SPH, sphere cultures; TAGs, triacylglycerols; DNL, de novo lipogenesis.

Conflicts of interest: The authors declare no competing interests

Financial support: Funding for this work was provided by grants from Associazione Italiana per la Ricerca sul Cancro (AIRC) (IG23117) to CR, (IG27094) to MLT, Cassa di Risparmio di Pistoia e Pescia, and the University of Florence to FM.

Dr. Andersen and Dr. Raggi are members of the European Network for the Study of Cholangiocarcinoma (ENSCCA) and participate in the initiative COST Action EURO-CHOLANGIO-NET granted by the COST Association (CA18122).

Ethical approval statement: The study was performed in accordance with the guidelines of the Helsinki Declaration.

Patient consent statement: Informed consent was obtained from all patients.

Permission to reproduce material from other sources: No materials reproduced from other sources in this manuscript.

Authors' contribution: CR, FM designed the study and wrote the manuscript. GL, MP, NN, BP, RB, ER, IT, ML, JBA, TL, AA, MLT, EP, CM, CA, SM, ES, SR, AT, GA, MR, PO, CPN, MP, FC, SS, AG provided materials, performed the experiments, collected the data, and analyzed the results. CR and MF supervised the project and critically revised the manuscript. All authors have read and approved the final manuscript.

Acknowledgments: The authors thank Dr. A.J. Demetris (University of Pittsburgh, Pittsburgh, PA, USA) for cholangiocarcinoma cell lines (HUCCT1 and CCLP1).

Data availability statement: The data that support the findings of this study are available from the corresponding authors [FM, CR], upon reasonable request.

Short Title: Fatty acids in cholangiocarcinoma stem-like cells

ABSTRACT

Background and Aims: Among reprogrammed metabolic pathways described in cancer stem cells, aberrant lipid metabolism has recently drawn increasing attention. Our study aimed to explore the contribution of fatty acids (FA) in the regulation of stem-like features in intrahepatic cholangiocarcinoma (iCCA).

Methods: We previously identified a functional stem-like subset in human iCCA by using a 3D sphere (SPH) model in comparison to parental cells grown as monolayer (MON). In this study, quantification of intracellular free FA and lipidomic analysis (triacylglycerol [TAG] composition, *de novo* synthesis products) were performed by LC-MS and LC-MS/QTOF, respectively, in both SPH and MON.

Results: Stem-like SPH showed a superior content of free FA (citric, palmitic, stearic and oleic acids) and unsaturated TAG. Molecularly, SPH showed upregulation of key metabolic enzymes of *de novo* FA biosynthesis (AceCS1, ACLY, ACAC, FASN, ACSL1) as well as of the mTOR signaling pathway. In iCCA patients (n=68), tissue expression levels of FASN, a key gene involved in FA synthesis, correlated with five-year overall survival. Interference with FASN activity in SPH cells through both specific gene silencing (siRNA) or pharmacological inhibition (orlistat) decreased sphere-forming ability and expression of stem-like markers. In a murine xenograft model obtained by injection of iCCA-SPH cells, FASN inhibition by orlistat or injection of FASN-silenced cells significantly reduced tumor growth and expression of stem-like genes.

Conclusion: An altered FA metabolism contributes to maintenance of a stem-like phenotype in iCCA. FASN inhibition may be a new potential approach to interfere with the progression of this deadly disease.

Impact and implications

Recent evidence indicates that metabolic disorders correlate with an increased susceptibility to intrahepatic cholangiocarcinoma (iCCA). Our investigation emphasizes the pivotal involvement of lipid metabolism in the tumor stem-cell biology of iCCA, facilitated by the upregulation of crucial enzymes and the mTOR signaling pathway. From a clinical perspective, this underscores FASN's dual role as both a prognostic indicator and a therapeutic target, suggesting that FASN inhibitors could enhance patient outcomes by diminishing stemness and tumor aggressiveness. These findings pave the way for novel therapeutic strategies for iCCA and shed light on its relationship with metabolic disorders such as diabetes, obesity, metabolic syndrome and MASLD.

INTRODUCTION

Stem cell programs in cancer initiation, progression, and therapy resistance are considered as the centerpiece of tumor biology. The identification of cancer stem cells (CSC) in many solid tumors, including hepatic cancer (1-3), has provided novel insight into the mechanisms of carcinogenesis. In CCA, the presence of stem-like cells has been correlated with more aggressive tumor characteristics and poorer patient prognosis (4). Investigation on CSC has been favored by the development of *in vitro* systems enriched in stem-like cells. At this regard, we and others have developed and employed 3D tumor sphere (SPH) formation as an efficient *in vitro* tool to enrich for stem-like cells (1-3).

Although studies on CSC biology have identified relevant signals sustaining tumor-stemness, the exploration of metabolic reprogramming in the control of the stem state is in its infancy. Novel lines of evidence are shedding light on the dependence of CSC on lipid metabolism and particularly on fatty acids (FA) (5-8). This emerging concept linking lipid metabolism and stem-cell fate mostly derives from studies assigning a CSC-promoting function to the excess of monounsaturated fatty acids (9, 10).

Recently, new experimental evidence, although divergent, has highlighted a role for lipid metabolism in the pathogenesis of CCA. In line with the histological and molecular heterogeneity of this neoplasm, highly proliferative CCA cells are strongly lipid-dependent, as shown by their up-regulated lipid and lipoprotein uptake and catabolism for proliferation. On the other hand, more advanced stages of disease or CCAs associated with C. sinensis infection appear to exhibit elevated expression of FASN. Furthermore, in lymph node metastases, CCA colonization appears to be driven by PPARγ-regulated lipid metabolic reprogramming (11-15).

Despite these recent lines of evidence, little is known about the role of lipids and lipid metabolism in iCCA-stemness. Here we show that altered fatty acid metabolism is a distinctive feature of tumor stem-like cells in iCCA.

RESULTS

Fatty acids enhance stemness features in iCCA cells

To assess the relevance of fatty acids (FA) in the biology of iCCA stem cells, CCLP1 and HUCCT1 cells were first exposed to increasing concentrations of unsaturated (oleic, palmitoleic, linoleic acids) or saturated (palmitic acid) FA for different time spans (Figure S1-2, Table S1-2). In line with previous studies (14), all tested FA promoted cell growth (Figure S1-2, Table S1-2). Thus, based on the highest effect (Figure S1-3), we focused our study on the role of oleic acid (OA) and palmitoleic acid (POA) in the modulation of iCCA stemness.

Since CSC are key players in tumorigenesis including tumor initiation and metastasis, we next evaluated whether FA are able to modulate these aspects *in vitro* by reprogramming parental cells grown in monolayer (MON). Indeed, treatment of MON cells (HUCCT1 or CCLP1) with OA or POA markedly enhanced their sphere-forming ability (i.e. sphere number, volume, and growth overtime)

as indication of self-renewal potential (Figure 1A, Figure S4A-B), significantly increased aldehyde dehydrogenase activity, serving as a functional marker of tumor stemness (Figure S4C) and the notably improved the capacity to invade a basement-like membrane (Figure 1B, Figure S5). Accordingly, expression levels of multiple genes implicated in the maintenance of stemness, self-renewal and regulation of epithelial-to-mesenchymal transition (EMT) were modulated in a pro-malignant fashion (Figure 1C), thus further supporting the *in vitro* functional importance of FA in acquiring a stem-like traits. On the other hand, due to their drug-resistance, cancer stem cells can escape cytotoxicity and survive chemotherapy and radiotherapy. Therefore, we assessed the influence of monounsaturated FA on iCCA resistance to chemotherapeutic agents. Pre-treatment with OA or POA before exposure to cisplatin, oxaliplatin and gemcitabine, commonly used drugs for iCCA therapy (1), led to a significant rescue of cell viability under pharmacological-treatment as shown by analysis of apoptosis (Figure 2, Figure S6, TableS3).

The fatty acid metabolic machinery is boosted in CCA stem-like cells

Based on the observed enrichment of stem cell properties *in vitro* in MON cells treated with exogenous OA or POA, we further investigated the metabolic apparatus of fatty acids in the 3D sphere (SPH) culture system. This system functions as a model of tumor stemness in CCA, as previously described by our group (1) and confirmed at the molecular level by RNA-sequencing profiling of SPH cells (FigureS7, Table S4). Utilizing Enrichr analysis, we observed a significant enrichment of stem-related molecules among the differentially expressed genes in SPH compared to MON across both cell lines. The acquisition of stemness is further supported by the predominant activation of stem cell signaling pathways, including PI3K-Akt, Hippo, and TGF-beta-dependent pathway. Additionally, there was an upregulation of significant networks associated with the EMT process, TNF-alpha signaling via NF-kB, the p53 pathway, as well as factors related to pluripotency, stemness, and EMT, such as POU5F1, STAT3, EZH2, ZEB1, MYC, SOX2, and ZEB2 (Figure S7, Table S4).

Gene set enrichment analysis (GSEA) of SPH RNA sequencing data indicated a marked increase in the expression of several genes participating in FA metabolism, including both anabolic and catabolic pathways (Figure 3A). In accordance, unsupervised clustering heat map indicated a primary divergence in expression pattern of differential expression genes involved in FA metabolism between SPH and MON for both cell lines (Figure 3B). Furthermore, overexpression of key enzymes involved in FA synthesis (FASN, SREB, ACSL1, SCD1), desaturation (SCD1), and exogenous uptake (CD36, FATP4) was further confirmed at mRNA levels in SPH cells compared to MON cells (Figure 3C). Of note, protein content of mTOR signaling pathway and key metabolic enzymes of *de novo* fatty acid biosynthesis (cytoplasmic acetyl-CoA synthetase (AceCS1), ATP citrate lyase (ACLY), Acetyl-CoA carboxylase (ACAC) the rate-limiting step in fatty acid synthesis, FASN, Acyl-

CoA synthetase long chain family member 1 (ACSL1) were up-regulated in SPH with respect to MON of both CCLP1 and HUCCT1 cells lines, as shown by western blot analysis with relative densitometric analysis (Figure 3D, Figure S8). Notably, it is well known that mTOR stimulates *de novo* lipogenesis via SREB dependent pathway throughout S6K phosphorylation (16).

Based on these evidence, content of selected intracellular free FAs in iCCA stem-like cells was next quantified by liquid chromatography mass spectrometry. Notably abundance of citric acid, the FA precursor as well as palmitic acid, stearic acid and oleic acid were revealed in SPH cells compared to respective MON in both cell lines (Figure 4) in accordance with molecular data (Figure 3) showing differences in expression of key enzymes of FA biosynthesis. Coherently, BODIPY staining showed that iCCA-SPH had a higher amount of lipid droplets which are dynamic organelles constituted mainly by triglycerides containing FA with different degree of saturation or size (i.e. number of carbons due to elongation) (Figure 5A-B).

Therefore, an untargeted lipidomic analysis was performed using high resolution mass spectrometry and targeted quantification of most relevant lipids. By comparing triglycerides amount and composition in SPH and the respective parental cells grown as monolayer, we observed that iCCA-SPH were characterized by a higher triacylglycerols (TAGs) with saturated and monounsaturated fatty acids (i.e. TAG with 1-2 double bonds) with respect to MON (data not shown). This was particularly evident in HUCCT1 although both SPH contain TAG with lower length than MON (i.e. TAG with less than 52 Carbons). Incubation with deuterated water was used to quantify contribution of fatty acids from *de novo* lipogenesis (DNL) to single triglycerides species. Palmitic acid (C16:0) is the main product of DNL and can either be desaturated to palmitoleic acid (C16:1) or elongated to stearic acid (C18:0) that in turn can be desaturated to oleic acid (C18:1). The iCCA-SPH exhibited a larger percentage of *de novo* synthesized triglycerides (Figure 5C), as assessed through the measurement of incorporation of deuterium. Within TAGs with lower length, SPH contained more TAG with monounsaturated triglycerides than MON, i.e., TAGs with palmitoleic and oleic fatty acids (48:1, 50:1, 52:1, than TAG incorporating only saturated FA like palmitic and stearic acid, (48:0, 50:0, 52:0), as shown in Figure 5C-D. Accordingly, the desaturation index, i.e. the ratio between triglycerides with one double bond in the FA chain and triglycerides without double bonds indicated a larger amount of monounsaturated FA in SPH (Figure S9).

We next evaluated the pathways responsible for fatty acid metabolism. SPH cells were characterized by elevated activity of intracellular fatty acid beta-oxidation (FAO) compared to MON (Figure S10). This observation is supported by the increased content in lipid droplets evident in CCA-SPH (Figure 5A-B). Collectively, these findings identify a distinct alteration in mitochondrial function within SPH compared to MON, corroborated by the previous study from our group (2). To provide a more comprehensive perspective, we explored the classification of CCA patients based on stemness and FA metabolic pathways in publicly available datasets (GSE32879 and GSE89749). Gene expression profiles for GSE89749 and GSE32879 were obtained from the gene expression omnibus. Curated

list of stemness and chemoresistance genes, as well as Gene Ontology fatty acid beta oxidation (FAO) and KEGG Biosynthesis of unsaturated fatty acids (DNL) were used in the analysis. Within each dataset, samples underwent z-scoring and hierarchical clustering based on the expression of stemness genes. Next, GSEA was used to establish association of clusters with chemoresistance, DNL and FAO. Hierarchical clustering allowed the clear definition of 2 clusters (A and B), based on the expression of 139 resistance and stemness genes (resistance&stemness signature). In each dataset, Cluster B was significantly enriched in expression of stemness and resistance genes that was validated with GSEA (Figure S11-12). In both GSE32879 and GSE89749 set, Cluster B was enriched in both FAO and DNL suggesting positive association of stemness and FAO and stemness and DNL. Taken together, these data suggest that the stem-like subset has an amplified machinery for fatty acid metabolism in iCCA.

Higher expression of FASN is associated with a more aggressive course in patients with iCCA

To explore the possible relevance of our *in vitro* data to the clinical setting, we analyzed transcriptomic data from a published cohort of patients with iCCA to search for possible correlations between genes implicated in FA metabolism and clinical outcomes (17). In particular, we focused our attention on FASN gene, the master regulator of fatty acids synthesis, which was upregulated in SPH compared to MON iCCA cells. Clustering data based on FASN expression level, Kaplan-Meyer curves demonstrated that higher FASN, was strongly associated with significantly lower survival (Figure 6A), in accordance with recently published data (13). Notably FASN levels correlated with available clinical pathological parameters (Table S5) in particular with portal trunck invasion, a significant adverse prognostic factor in iCCA (Figure 6B). In addition, FASN expression significantly correlated with a number of stemness-related genes including SOX2, NOTCH1 and ABCG2 in the same iCCA dataset (n=68) (Figure 6C).

FASN promotes the growth of experimental iCCA and confers stem cell features to the tumor

Based on the results of transcriptomic analysis in patients, we next investigated the effect of genetic (siRNA) or pharmacological inhibition of FASN in SPH cells. Drug inhibition was performed by using orlistat, an anti-obesity drug that irreversibly inhibits the enzymatic activity of FASN (18-22). Both specific genetic depletion (siRNA) (Figure S13) or enzymatic inhibition (orlistat) of FASN in SPH cells significantly reduced *in vitro* functionally properties such as proliferation, sphere-forming ability, invasion as well drug-resistance (13) (Figure 7A-C; Figure S13-14).

Molecularly, FASN reduction impaired the expression of several key genes implicated in pluripotency (i.e. NANOG, SOX2, KLF4, OCT4, BMI1), drug-resistance (ABC transporters) and EMT (CHD2, VIM, ZEB1, ZEB2, SNAI1), and impact the phosphorylation of pro-survival proteins (i.e. AKT, p38 and ERK1/2) as well as expression MYC oncoprotein (Figure 7D-E).

Based on the strong *in vitro* data indicating the involvement of FASN in the features of iCCA stem compartment relevant for tumor progression, we evaluated the possible impact of the inhibition of this protein in an *in vivo* model of CCA. To this aim, the effect of both orlistat pharmacological treatment and genetic FASN inhibition (shRNA) was investigated in a mouse xenograft model in which dissociated CCLP1 SPH cells were injected subcutaneously in flank(s) of NOD/SCID mice (2).

After confirming that treatment with orlistat at a dose of 240 mg/kg/day was not toxic (FigureS15A) and in accordance with previously reported studies (18, 21, 22), mice were randomized once the tumor was palpable and treated with orlistat via i.p. injection (SPH-T ORL) or vehicle (SPH-T CTR) for 4 weeks. In parallel, we performed subcutaneous xenografts using CCLP1 cells silenced for FASN (SPH-T shFASN) or cells transfected with shCTR (SPH-T shCTR) after confirming FASN depletion at protein level (Figure S15B). Tumor growth was monitored with a dedicated *in vivo* imaging system. Tumor volume and weight in the ORL-treated and shFASN group were significantly reduced compared with SPH-T CTR and SPH-T shCTR, respectively (Figure 8A-B, FigureS15C), while no differences in liver/body weight and lung/body weight ratios were observed (Figure S15D-E). At the end of treatment, *in vivo* cell proliferation was evaluated by PCNA staining (Figure 8C). Both SPH-T ORL and SPH-T shFASN showed a lower number of cycling cells, in agreement with the observed impact on tumor progression. Moreover, comparison of the molecular characteristics of the xenografts (Figure 8D-E) showed in both SPH-T ORL and SPH-T shFASN tissues a downregulation of genes involved in proliferation (i.e. STAT3, MTDH, BCL2L1, XIAP, AKT, EGF, EGFR, E2F1, HGF, HRAS, IGF2, NRAS, PDGFRA, FZD7, PTK2, c-MYC), invasion (i.e. ZEB1, SLUG, Ncadherin, betacatenin, ADAM17, CXCR4, FDZ7,MET,PTK2), drug-resistance (ABCG2, ABCF1, ABCC2) and pluripotency (NANOG, NOTCH, HNF4, KLF4), cancer stem cell markers (CD44, CD13, EpCAM) together with upregulation of tumor-suppressor (i.e. OPCML, TP53, HHIP, SMAD4, RB1, GADD45B, PTEN, SFRP2, SOCS3) and proapoptotic genes (i.e. FADD, CASP8, BAX,BUD, TNFRSF10B) (Figure 8E).

Accordingly, at the protein level, FASN inhibition and depletion was associated with a lower activation/expression of proteins involved in proliferation or survival (i.e. STAT3, AKT, ERK1/2, c-MYC) and anabolic pathways (mTOR and PPARɣ) (Figure 8F), confirming the key role of FASN and FA metabolism in tumor growth.

MATERIALS AND METHODS

Metabolites extraction

For MON cell culture, cells in a 6 well-plate were quickly rinsed with NaCl 0.9% and quenched with 500 µl ice-cold 70:30 acetonitrile:water. Plates were placed at - 80 ◦C for 10 min, then cells were collected by scraping and sonicated 5 s for 5 pulses at 70% power twice. For SPH cell culture, 48 spheroids were collected from a 96-well plate for each sample and centrifuged at 600 rpm for 5 mins at 4°C. Pellets were washed with 1 ml of NaCl 0.9%, centrifuged as above and resuspended in 500 µl ice-cold 70:30 acetonitrile:water. Samples were placed at - 80 ◦C for 10 min and then sonicated 5 s for 5 pulses at 70% power twice. At this point, for both MON and SPH experiments, samples were centrifuged at 12000g for 10 min and supernatants were collected in a glass insert and dried in a centrifugal vacuum concentrator (Concentrator plus/Vacufuge plus, Eppendorf) at 30 °C for about 2.5 h. Samples were then resuspended with 150 µl H2O prior to analyses.

Liquid Chromatography-Mass Spectrometry (LC-MS) analysis

LC separation was performed using an Agilent 1290 Infinity UHPLC system and an InfintyLab Poroshell 120 PFP column (2.1 × 100 mm, 2.7 µm; Agilent Technologies). Mobile phase A was water with 0.1% formic acid. Mobile phase B was acetonitrile with 0.1% formic acid. The injection volume was 10 µL and LC gradient conditions were: 0 min: 100% A; 2 min: 100% A; 4 min: 99% A; 10 min: 98% A; 11 min: 70% A; 15 min: 70% A; 16 min: 100% A with 2 min of post-run. Flow rate was 0.2 ml/ min and column temperature was 35 ◦C. MS detection was performed using an Agilent 6550 iFunnel Q-TOF mass spectrometer with Dual JetStream source operating in negative ionization mode. MS parameters were: gas temp: 285 ◦C; gas flow: 14 l/min; nebulizer pressure: 45 psig; sheath gas temp: 330 ◦C; sheath gas flow: 12 l/min; VCap: 3700 V; Fragmentor: 175 V; Skimmer: 65 V; Octopole RF: 750 V. Active reference mass correction was done through a second nebulizer using masses with m/z: 112.9855 and 1033.9881. Data were acquired from m/z 60–1050. Data analysis and isotopic natural abundance correction were performed using MassHunter Profinder (version 10.0.2). Data preprocessing was performed using the Batch Targeted Feature Extraction algorithm and Agile 2 algorithm. This software assigned identities to metabolites by searching against an in-house compound database built with Agilent PCDL Manager (version B.08.00) based on the metabolite formula and its corresponding retention time with a score > 75. Peak areas obtained were normalized for protein content for each sample. LC-MS analysis was performed by the Metabolomics Unit of JRU ISBE-SYSBIO Center and Elixir European Infrastructure in Milan (Milan, Italy).

In vivo experiment

Animal experiments were performed in accordance with national guidelines and approved by the ethical committee of the Animal Welfare Office of Italian Health Ministry. All procedures conformed to the legal mandates and the Italian guidelines for the care and maintenance of laboratory animals. All animals received human care and study protocols comply with the institution's guidelines. Studies involving animal experiments conform to the Animal Research: Reporting of In Vivo Experiments (ARRIVE) guidelines (http://www.nc3rs.org.uk/arriveguidelines), developed by the National Centre for the Replacement, Refinement and Reduction of Animals in Research (NC3Rs) to improve standards and reporting of animal research. Male NOD/SCID mice (n=6 per group) of six weeks (Charles River Laboratories International) were subcutaneous injected with $3x10^6$ CCLP1 SPH cells. When tumor became palpable mice were randomly divided in two experimental groups to receive intra-peritoneal injection of solution (10% DMSO, 40% PEG300, 5% TWEEN80 and 45% saline) or 240mg/Kg orlistat (three times a week). Animals were monitored daily. In parallel, we performed subcutaneous xenografts using injected CCLP1 cells ($3x10^6$) silenced for FASN (SPH-T shFASN) or cells transfected with shCTR (SPH-T shCTR) (male NOD/SCID mice (n=6 per group) of six weeks (Charles River Laboratories International).

Statistical analysis

Suitable statistical tests were performed using GraphPad Prism 9 software and R version 4.1.0. For each experiment, statistical details can be found in the figure legends, including statistical tests and sample sizes. All *in vitro* experiments were confirmed by independent biological replicates. Data is represented as mean ± SD or ± SEM. Significance levels are as follows: *p≤0.05, **p≤0.01, ***p≤0.001. Group comparison was performed using the nonparametric Mann-Whitney U test. Clinical data were examined using Fisher's exact test. The Kaplan- Meier method was employed to determine survival rates, with significance assessed using the Log-rank test. Pearson correlation was utilized to assess the relationship between gene expressions.

Detailed information is provided in the Supporting Information and in the Supplementary CTAT Table.

DISCUSSION

Metabolic rewiring is a new hallmark of cancer, and in recent years information on this topic has changed the view of tumor biology. Among several tumor metabolic alterations, lipid metabolism is receiving increasing attention, and several studies have demonstrated its central role in the process of carcinogenesis (23). As major components of lipids, FA provide energy, membrane building

blocks, signaling molecules and post-translational modifications of proteins which are determinants for cancer cell survival.

The present study provides several lines of information on the role of increased FA metabolism in conferring a stem-like phenotype in iCCA. Notably, exposure to monounsaturated FA increased stem-like features at both functional (resistance to antineoplastic drugs, spherogenicity) and molecular (expression of stemness-associated genes) level. Taking advantage of a 3D SPH culture system as a model for cancer stem cells (1, 2), and comparing these cultures with more differentiated parental cells grown in monolayers, we provide compelling evidence for the importance of fatty acids in the regulation of the stemness features of iCCA. Several key enzymes involved in FA synthesis and transport were significantly overexpressed in the iCCA stem-compartment, indicating that a CSC phenotype is strictly associated with altered FA metabolism. Additionally, lipidomic analysis demonstrated that iCCA-SPH exhibit a higher *de novo* synthesis and desaturation FA that are then esterified to triglycerides that results enriched in monosaturated fatty acids. This finding may suggest that *de novo* synthesis and desaturation of FA may have an essential role in fueling the activation of pluripotency and self-renewal associated signaling networks contributing either reprogramming iCCA cells towards a less differentiated stem-like phenotype or favoring the expansion of the stem subpopulation by supporting their metabolism. In line with our results, a recently published study (14) highlighted the pathogenic role of fatty acids, showing that exogenous supply of FA modulated the growth of CCA cells. Unlike more differentiated tumor cells, enhanced FA biosynthetic apparatus of iCCA stem-like cells probably render them more independent from the external source.

Additionally, increased expression of FASN, the key enzyme in FA synthesis, was correlated with shorter survival in a dataset of 68 iCCA patients thus suggesting that tumors with a worse prognosis are characterized with an increased content of intracellular fatty acids. This might be potentially interesting considering our *in vitro* evidence of increased drug-resistance after exposure fatty acids. However, a detailed analysis of the underlying molecular mechanism(s) FA-driven is needed to provide the base knowledge for effective acquisition of a pharmacologically resistant iCCA phenotype.

Nevertheless, we went further to demonstrate the functional relevance of FASN in stem-like iCCA cells both in the *in vitro* and *in vivo* settings. *In vitro*, FASN inhibition with both orlistat and a specific gene silencing induced a significant decrease in pluripotency and stemness markers, as well as in the expression of genes involved in EMT and drug-resistance. These effects were replicated in a preclinical model of iCCA *in vivo*, where FASN inhibition caused a significant reduction in tumor growth after injection of resuspended iCCA-SPH. This was associated with dramatic changes in the expression of genes related to stemness and aggressiveness of iCCA. These data, together with those obtained in patients with iCCA, collectively indicate that tumor stem-like cells have distinct

rearrangements of FA metabolism compared to more differentiated cells, and metabolic rewiring contributes to self-renewal and stemness maintenance with a major impact on the aggressiveness of iCCA cells.

Although the development and progression of cancer are frequently associated with increased *de novo* production of fatty acids in several tumor types, the role of FASN in CCA is still controversial (12-15). Indeed, several studies (12), have shown that cholangiocarcinogenesis can be insensitive to FASN deprivation since CCA cells displayed enhanced fatty acid uptake-related machinery. Differences observed in various studies may be ascribed to variances in patient cohorts, including different underlying etiological factors (e.g., higher prevalence of MASLD, metabolic syndrome, or diabetes) and the intricate dynamics of the tumor microenvironment, especially the immune milieu. Furthermore, the diversity between liver tumor populations may result in variable reliance on FASN across cellular subsets. An additional explanation for these apparently divergent results can be that enhanced *de novo* lipogenesis and increased FASN expression are strictly related to the stemness component rather than to the more differentiated iCCA cells. Moreover, the abnormally activated *de novo* synthesis of FA may contribute to satisfy the energy needs for the maintenance of a stemness state in iCCA, as also suggested by our previous study (2). Thus, our results identify a new player in the regulation of lipid metabolism in iCCA with particular relevance to the biology of the stem cell compartment, and which could represent a target for treatment to be explored in dedicated studies. Of note, new FASN inhibitors are being developed, including TVB-2640, already used in clinical trials for the treatment of MASLD (24).

An important aspect that will deserve additional research is relate to the possible interaction beween altered FA metabolism and metabolic disorders, such as MASLD, which are associated with an elevated risk of iCCA (25-28).

Recently, it has been shown that metabolic disorders are associated with an elevated risk of intrahepatic CCA (25-28). These metabolic risk factors encompass diabetes, obesity, metabolic syndrome and MASLD, which are frequently associated with dyslipidemia. Unfortunately, the current datasets including clinical data do not specifically report the presence of MASLD, metabolic syndrome, or diabetes. However, it is imperative to investigate the potential presence and role of increased stemness in iCCA patients with these comorbidities. Further exploration and additional clinical data encompassing these specific aspects are warranted.

In conclusion, this study provides evidence that an altered fatty acid metabolism contributes to the maintenance of stem-like phenotype in iCCA. These data allow to better understand the biology of CSCs in iCCA and suggest that inhibition of FASN may be a new potential target to interfere with tumor initiation of this deadly disease.

Figure Legends

Figure 1. Effects of monounsaturated FAs on stem-like proprieties in iCCA cells. (A) Intrahepatic CCA cells were grown as spheres for seven days, in presence or absence of FAs. Then SPH were counted, and their volume measured. Mean ± SEM (n=3, ***p≤0.001). Representative images of iCCA SPH are reported below the graphs (original magnification 40X). (B) Migration of iCCA cells was measured in modified Boyden chambers, after 48 hours treatment. Mean ± SEM (n=3, ***p≤0.001). Representative images of filters are shown below the barograms (original magnification 40x, scale bar 10μM). (C) Expression of different genes involved in EMT, drug-resistance and stem like acquisition in CCLP1 and HUCCT1 cells were treated with OA or POA for 48h, reported as fold changes normalized to mean expression of vehicle treated cells. Mean ± SEM (n=3, *p≤0.05, **p≤0.01, ***p≤0.001; Mann-Whitney U test).

Figure 2. Monounsaturated FAs pretreatment protects iCCA cells from antiblastic toxic effects. CCLP1 and HUCCT1 cells were pretreated for 24 hours with oleic acid (OA) or palmitoleic acid (POA) in starvation medium, then with (A) cisplatin, (B) oxaliplatin or (C) gemcitabine for further 24 hours. Apoptosis was measured with Annexin V/PI staining. Data are mean ± SEM (n=3, ***p≤0.001, $\oint$ p≤0.05, $\oint\oint$ p≤0.01, $\oint\oint\oint$ p≤0.001; Mann-Whitney U test). The * are calculated respect to cisplatin, oxalilplatin or gemcitabine, $\oint$ are calculated respect to vehicle. Complete statistical data are shown in Table S3.

Figure 3. Molecular aspects behind altered FA pathways in iCCA stem-like cells. (A) Results of a GSEA Pre-ranked analysis on the fatty acids metabolism gene set of the Hallmark MSigDB collection. (B) Heatmap plot of differentially expressed genes of the genes involved in fatty acid metabolism in spheres (SPH) and monolayers (MON), using Euclidean distance as similarity metrics and complete linkage as linkage method. Modified Zscores of the individual genes, as median-centered log2 intensity values divided by standard deviation, are shown by a blue-to-red gradient variation. Different colors specified different FA metabolic pathways. (C) CCLP1 and HUCCT1 cells were grown as monolayer (MON) or as spheres (SPH), then RNA was extracted. Expression of different genes involved in FA metabolism is reported as fold changes normalized to mean expression of MON. Mean ± SEM (n=3, *p≤0,05, ** p≤0,01, *** p≤0,001; Mann-Whitney U test). (D)Representative immunoblot of mTOR, phosho mTOR, S6K, phosphoS6K, AceCS1, ACLY, ACAC, FASN, ACSL1 protein levels in CCLP1 and HUCCT1 cells grown as MON and SPH. β-Actin immunoblot was performed to ensure equal loading. ES, enrichment score; FA, Fatty Acids; FDR, false discovery rate; GSEA, gene set enrichment analysis; MFI, mean fluorescent intensity; NES, normalized enrichment score.

Figure 4. Content of free fatty acid in iCCA stem-like compartment. Relative metabolite abundance of intracellular free citric, stearic, oleic and palmitic acid in CCLP1 or HUCCT1 cell lines, grown in monolayer (MON) or as spheroids (SPH), identified by LC-MS analysis. Peak areas obtained were normalized for protein content for each sample. Mean ± SEM (n=9, ** p≤0,01, *** p≤0,001; Mann-Whitney U test).

Figure 5. Triglycerides composition in iCCA cells grown as monolayer or spheres. (A) Intrahepatic CCA cells were grown as monolayer (MON) or sphere (SPH), then cells were stained with Bodipy 493/503. Confocal microscopy analysis of lipid droplets in MON and SPH. (light yellow: Bodipy 493/503; blue: Hoechst; scale bar = 5μm). (B) Lipid droplets quantification by cytofluorimetric analysis. Histograms represent the MFI of the Bodipy probe normalized to mean MFI of MON. Results are mean ± SEM (n=3, **p≤0.01, *** p≤0.001; Mann-Whitney U test). (C) Representation of triglycerides concentration in CCLP1 and HUCCT1 grown as MON or SPH, respectively. Single triglycerides were identified according to their degree of saturation (x axis) i.e., the number of double bonds, and elongation number (y axis) i.e., the number of carbons. Triglycerides concentrations were scaled to zero mean and unit variance and reported as median for each cell line grown as MON or SPH. (D) Concentration of the main saturated triglycerides (TAG) and their desaturated counterpart in CCLP1 MON (blue), SPH (green), HUCCT1 MON (red), SPH (orange) cultured cells, respectively. The measured concentrations are composed by two parts: the de novo synthesized component, characterized by deuterium incorporation levels ranging from 1 to 5 (M1-M5) and displayed in lighter shades, and the pre-existing component that was not newly synthesized i.e., without any incorporation of deuterium (M0), and is depicted in darker tones. In table, molar percents of de novo synthesized TAG, measured as deuterium enrichment after D2O incubation, were reported. * p<0.05 ; nonparametric test of the Mann Whitney ranks.

Figure 6. Expression of Fatty Acid Synthase is associated with poor survival in iCCA patients. (A). Kaplan-Meyer plot showing overall survival in iCCA patients (n=68) stratified according to good or bad prognosis. (B)The univariate association of FASN expression with clinical pathological parameters (C) Scatterplot representing the correlation between FASN and SOX2, NOTCH, ABCG2 and VEGF expression in a public dataset (17).

Figure 7. Effects of FASN depletion in CCLP1 SPH. (A) Effect of FASN depletion on proliferation by BrdU incorporation 48 hours after orlistat treatment (upper panel) or gene silencing (lower panel). Mean ± SEM (n=3, ***p≤0.001). (B) Effects of orlistat (upper panel) or FASN gene silencing (lower panel) on iCCA sphere forming efficiency. Mean ± SEM (n=3, ***p≤0.001; Mann-Whitney U test). Representative images of iCCA SPH are reported below the graphs (original magnification 40X). (C)

Migration of orlistat treated SPH (upper panel) or FASN silenced SPH (lower panel) was measured in modified Boyden chambers. The number of migrated cells is represented as fold increase respect to vehicle. Mean ± SEM (n=3, ***p≤0.001; Mann-Whitney U test). Representative images of filters are shown below the barograms (original magnification 40x). (D) Expression of different genes involved in CSCs pathways, EMT and drug resistance expressed as fold changes normalized to mean expression of respective vehicle. Mean ± SEM (n=3, *p≤0,05, ** p≤0,01, *** p≤0,001; Mann-Whitney U test). (E) Immunoblot of several proteins and phosphoproteins involved in cell proliferation and survival, following orlistat treatment or FASN silencing. β-Actin immunoblot was performed to ensure equal loading.

Figure 8. Effects of orlistat treatment in iCCA xenografts mouse model. (A) Analysis of tumor volume by Vevo LAZR-X photoacoustic imaging. Tumors (SPH-T) were obtained by subcutaneous injection of SPH cells in NOD/SCID mice. Mice were treated with vehicle (SPH-T CTR) or orlistat (240mg/kg/day) (SPH-T ORL) (n = 6 per group) or injected with FASN silenced SPH cells (SPH-T shFASN) or cells transfected with shCTR (SPH-T shCTR) (ϕϕϕ p≤0.001 SPH-T ORL vs SPH-T CTR; SPH-T shFASN vs SPH-T shCTR ***, p≤0.001; Mann-Whitney U test). (B) Ultrasound images of representative subcutaneous tumor masses derived from injection of CCLP1 SPH generated tumors in different conditions. 3D rendering of the tumor mass is shown in the inset. (C) PCNA and hematoxylin eosin co-staining by immunohistochemical analysis. Representative stainings are shown below the histogram. Ki67 positive nuclei are in brown color (***p≤0.001; Mann-Whitney U test). (D-E) Heatmap of different tumor samples based on qRT-PCR of arrays of genes focused on liver cancer pathways (84 genes) or cancer stem-like markers (31 genes). Gene expression levels are expressed as log2 transformed values in color code from blue (low) to orange (high) according to the color key scale bar. Hierarchical clustering was based on complete linkage on euclidean distances between genes (rows) or samples (columns). F) Immunoblot of several proteins involved in proliferation and survival in tumor samples. Vinculin immunoblot was performed to ensure equal loading.

References

Author names in bold designated shared co-first authorship

1. **Raggi C, Correnti M**, Sica A, et al. Cholangiocarcinoma stem-like subset shapes tumor-initiating niche by educating associated macrophages. J Hepatol 2017;66:102-115.

2. Raggi C, Taddei ML, Sacco E, et al. Mitochondrial oxidative metabolism contributes to a cancer stem cell phenotype in cholangiocarcinoma. J Hepatol 2021;74:1373-1385.
3. Raggi C, Factor VM, Seo D, et al. Epigenetic reprogramming modulates malignant properties of human liver cancer. Hepatology 2014;59:2251-2262.
4. Banales JM, Marin JJG, Lamarca A, et al. Cholangiocarcinoma 2020: the next horizon in mechanisms and management. Nat Rev Gastroenterol Hepatol 2020;17:557-588.
5. **Kuo CY, Ann DK.** When fats commit crimes: fatty acid metabolism, cancer stemness and therapeutic resistance. Cancer Commun (Lond) 2018;38:47.
6. Mancini R, Noto A, Pisanu ME, et al. Metabolic features of cancer stem cells: the emerging role of lipid metabolism. Oncogene 2018;37:2367-2378.
7. Yi M, Li J, Chen S, et al. Emerging role of lipid metabolism alterations in Cancer stem cells. J Exp Clin Cancer Res 2018;37:118.
8. Begicevic RR, Arfuso F, Falasca M. Bioactive lipids in cancer stem cells. World J Stem Cells 2019;11:693-704.
9. Noto A, De Vitis C, Pisanu ME, et al. Stearoyl-CoA-desaturase 1 regulates lung cancer stemness via stabilization and nuclear localization of YAP/TAZ. Oncogene 2017;36:4573-4584.
10. **Li J, Condello S**, Thomes-Pepin J, et al. Lipid Desaturation Is a Metabolic Marker and Therapeutic Target of Ovarian Cancer Stem Cells. Cell Stem Cell 2017;20:303-314.e305.
11. **Zhang H, Zhu K**, Zhang R, et al. Oleic acid-PPARγ-FABP4 loop fuels cholangiocarcinoma colonization in lymph node metastases microenvironment. Hepatology 2024.
12. **Li L, Che L**, Tharp KM, et al. Differential requirement for de novo lipogenesis in cholangiocarcinoma and hepatocellular carcinoma of mice and humans. Hepatology 2016;63:1900-1913.
13. Tomacha J, Dokduang H, Padthaisong S, et al. Targeting Fatty Acid Synthase Modulates Metabolic Pathways and Inhibits Cholangiocarcinoma Cell Progression. Front Pharmacol 2021;12:696961.
14. Ruiz de Gauna M, Biancaniello F, González-Romero F, et al. Cholangiocarcinoma progression depends on the uptake and metabolization of extracellular lipids. Hepatology 2022.
15. **Xu L, Zhang Y, Lin Z, Deng X,** et al. FASN-mediated fatty acid biosynthesis remodels immune environment in Clonorchis sinensis infection-related intrahepatic cholangiocarcinoma. J Hepatol 2024.
16. Peterson TR, Sengupta SS, Harris TE, et al. mTOR complex 1 regulates lipin 1 localization to control the SREBP pathway. Cell 2011;146:408-420.
17. Andersen JB, Spee B, Blechacz BR, et al. Genomic and genetic characterization of cholangiocarcinoma identifies therapeutic targets for tyrosine kinase inhibitors. Gastroenterology 2012;142:1021-1031.e1015.
18. **Kridel SJ, Axelrod F**, Rozenkrantz N, et al. Orlistat is a novel inhibitor of fatty acid synthase with antitumor activity. Cancer Res 2004;64:2070-2075.
19. **Peng H, Wang Q**, Qi X, et al. Orlistat induces apoptosis and protective autophagy in ovarian cancer cells: involvement of Akt-mTOR-mediated signaling pathway. Arch Gynecol Obstet 2018;298:597-605.
20. **Zhang Q, Zhou Y, Feng X, Gao Y, et al**. Low-dose orlistat promotes the therapeutic effect of oxaliplatin in colorectal cancer. Biomed Pharmacother 2022;153:113426.
21. **Zhang C, Sheng L, Yuan M**, et al. Orlistat delays hepatocarcinogenesis in mice with hepatic co-activation of AKT and c-Met. Toxicol Appl Pharmacol 2020;392:114918.
22. **Seguin F, Carvalho MA,** Bastos DC, et al. The fatty acid synthase inhibitor orlistat reduces experimental metastases and angiogenesis in B16-F10 melanomas. Br J Cancer 2012;107:977-987.
23. Baenke F, Peck B, Miess H, et al. Hooked on fat: the role of lipid synthesis in cancer metabolism and tumour development. Dis Model Mech 2013;6:1353-1363.

24. Loomba R, Mohseni R, Lucas KJ, et al. TVB-2640 (FASN Inhibitor) for the Treatment of Nonalcoholic Steatohepatitis: FASCINATE-1, a Randomized, Placebo-Controlled Phase 2a Trial. Gastroenterology 2021;161:1475-1486.
25. **Da Fonseca LG, Hashizume PH**, de Oliveira IS, et al. Association between Metabolic Disorders and Cholangiocarcinoma: Impact of a Postulated Risk Factor with Rising Incidence. Cancers (Basel) 2022;14.
26. **Park JH, Hong JY**, Park YS, et al. Persistent status of metabolic syndrome and risk of cholangiocarcinoma: A Korean nationwide population-based cohort study. Eur J Cancer 2021;155:97-105.
27. **Yugawa K, Itoh S**, Iseda N, et al. Obesity is a risk factor for intrahepatic cholangiocarcinoma progression associated with alterations of metabolic activity and immune status. Sci Rep 2021;11:5845.
28. **Cadamuro M, Sarcognato S**, Camerotto R, et al. Intrahepatic Cholangiocarcinoma Developing in Patients with Metabolic Syndrome Is Characterized by Osteopontin Overexpression in the Tumor Stroma. Int J Mol Sci 2023;24.

JHEP|Reports

JHEP Reports

CTAT methods

Tables for a "Complete, Transparent, Accurate and Timely account" (CTAT) are now mandatory for all revised submissions. The aim is to enhance the reproducibility of methods.

- Only include the parts relevant to your study
- Refer to the CTAT in the main text as 'Supplementary CTAT Table'
- Do not add subheadings
- Add as many rows as needed to include all information
- Only include one item per row

If the CTAT form is not relevant to your study, please outline the reasons why:

1.1 Antibodies

Name	Citation	Supplier	Cat no.	Clone no.
Phospho AKT (Ser473)		Cell Signaling Technology	#9271	
AKT		Cell Signaling Technology	#9272	
Phospho STAT3 (Y705)		Cell Signaling Technology	#9145	
STAT3		Cell Signaling Technology	#30835	
Phospho ERK1/2 (Thr2020/Y204)		Cell Signaling Technology	#9101	
ERK1/2		Cell Signaling Technology	#4348	
Phospho P38 (Thr180/Y182)		Cell Signaling Technology	#4511	
P38		Abcam	ab59461	
cMYC		Cell Signaling Technology	#5605	
P27		Cell Signaling Technology	#3686	
P21		Cell Signaling Technology	#2947	
FASN		Cell Signaling Technology	#3180	
AceCS1		Cell Signaling Technology	#3658	
ACSL1		Cell Signaling Technology	#9189	
ACAC		Cell Signaling Technology	#3666	
ACLY		Cell Signaling Technology	#4332	
PPARγ		Cell Signaling Technology	#2430	
Phospho mTOR (Ser2448)		Cell Signaling Technology	#2971	
mTOR		Cell Signaling Technology	#2983	
Phospho S6K (Thr689)		Cell Signaling Technology	#9205	
S6K		Cell Signaling Technology	#9202	
β-actin		Merck	A5441	
Vinculin		Merck	V9131	
PCNA		Cell Signaling Technology	#2586	

JHEP|Reports

1.2 Cell lines

Name	Citation	Supplier	Cat no.	Passage no.	Authentication test method
CCLP1		kind gift from Dr. A.J. Demetris			
HUCCT1		kind gift from Dr. A.J. Demetris			
SG231		kind gift from Dr. A.J. Demetris			
iCCA4		Kind gift of Dr. V. Cardinale			

1.3 Organisms

Name	Citation	Supplier	Strain	Sex	Age	Overall n number

1.4 Sequence based reagents

Name	Sequence	Supplier

1.5 Biological samples

Description	Source	Identifier

1.6 Deposited data

Name of repository	Identifier	Link

1.7 Software

Software name	Manufacturer	Version
GraphPad Prism	GraphPad Software	ver.6

1.8 Other (*e.g.* drugs, proteins, vectors etc.)

Name	Supplier	Cat.no
Orlistat	MedChem Express	HY-B0218
QuantiNova LNA PCR	Qiagen	#SBHS-133ZE

JHEP|Reports

Focus Panels 384-well plates		
shFASN	Origene	TR313058
ALDH Assay kit	Merck	MAK082
Annexin V PI staining kit	Roche	11858777001
BrdU Proliferation Assay	Roche	11647229001
BODIPY 493/503	Cayman Chemicals	25892
FAO assay kit	Assay Genie	BR00001

1.9 Please provide the details of the corresponding methods author for the manuscript:

Chiara Raggi

2.0 Please confirm for randomised controlled trials all versions of the clinical protocol are included in the submission. These will be published online as supplementary information.

Figure 1

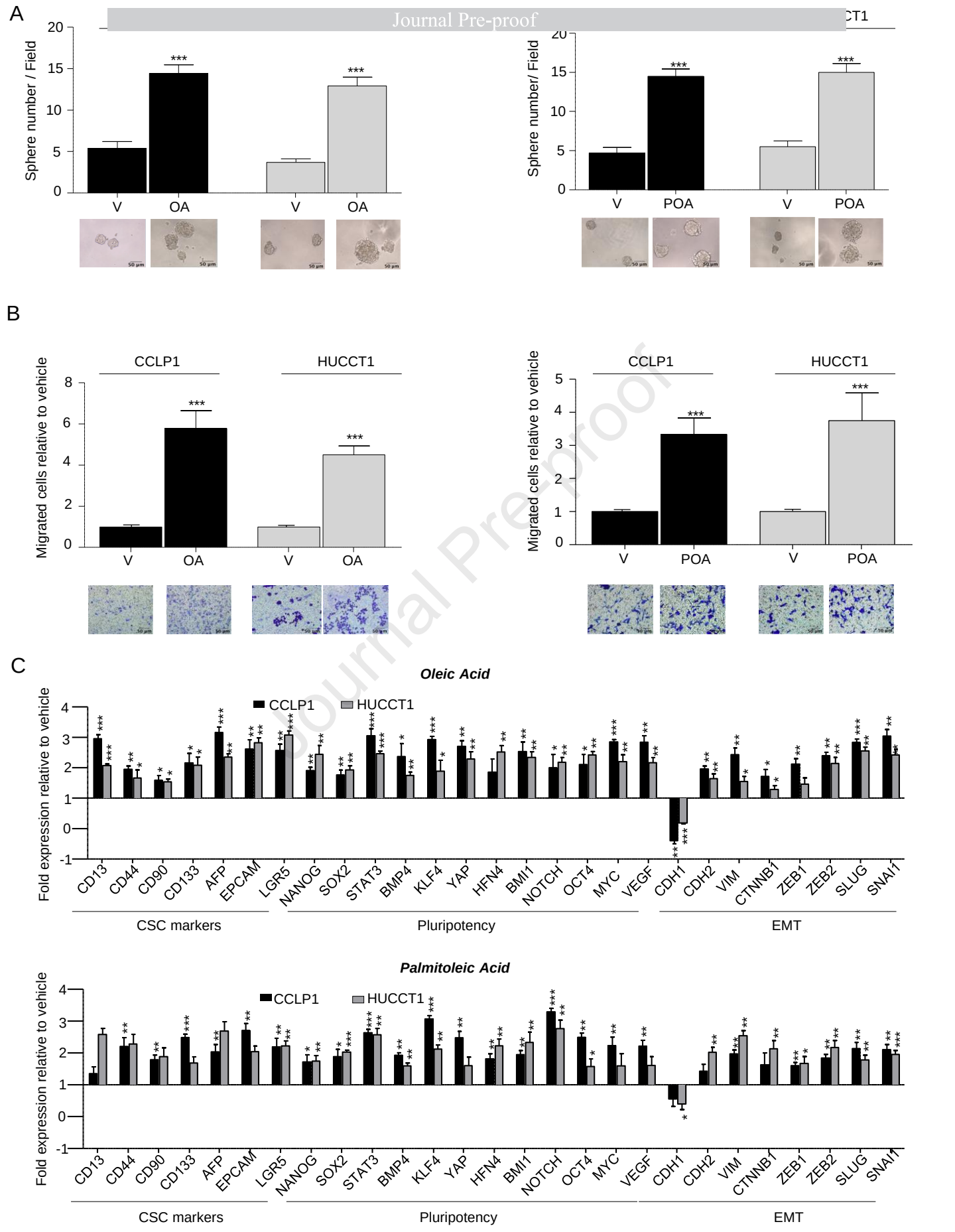

Figure 2

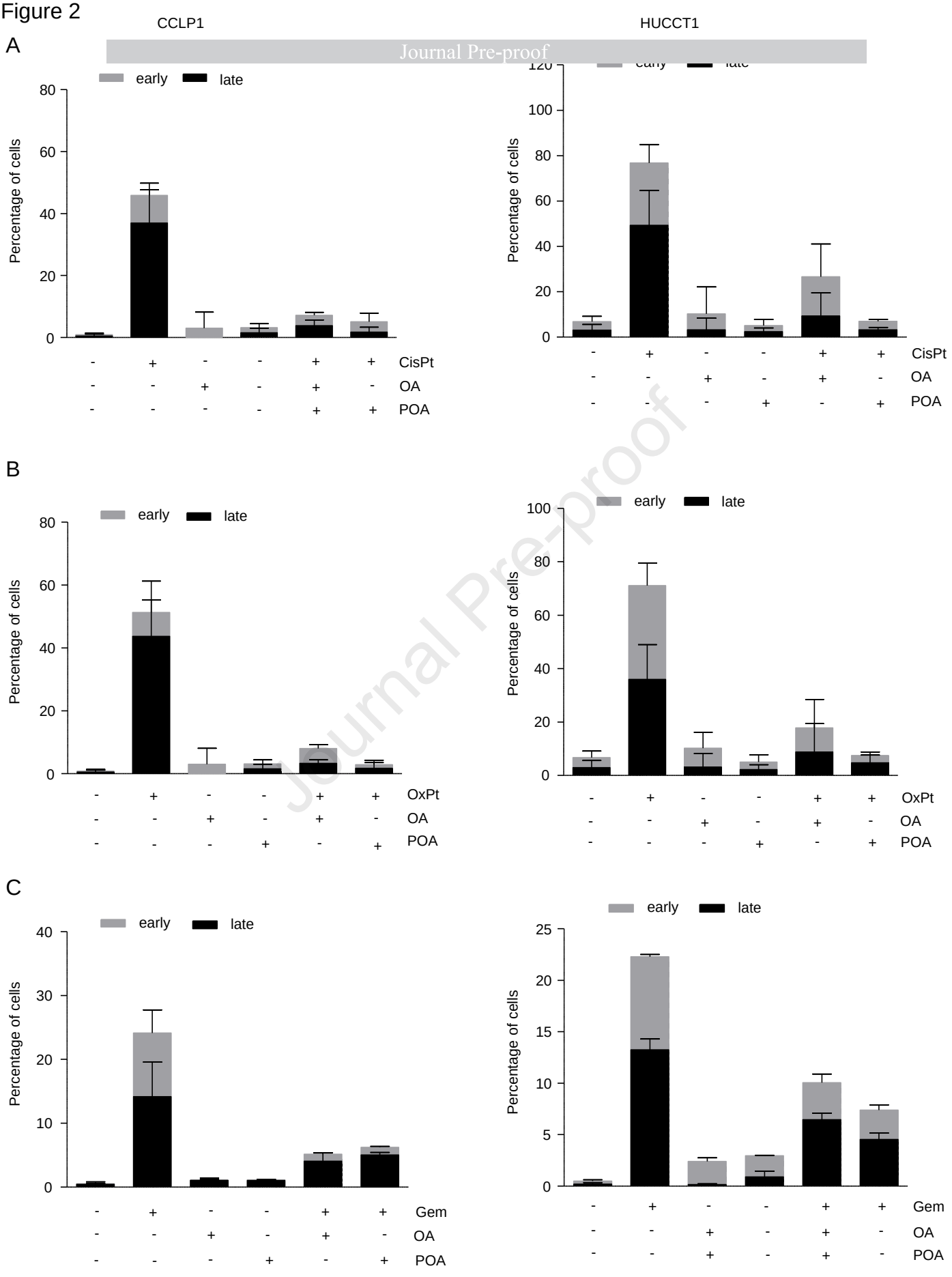

Figure 3

A

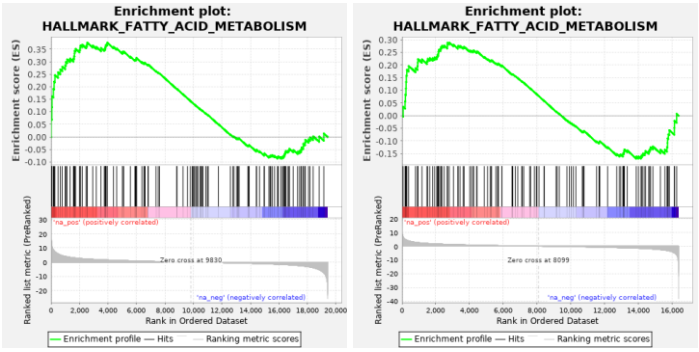

	ES	NES	FDR q-VAL
CCLP1 SPH	0.288	1.153	0.285
HUCCT1 SPH	0.376	1.393	0.042

B

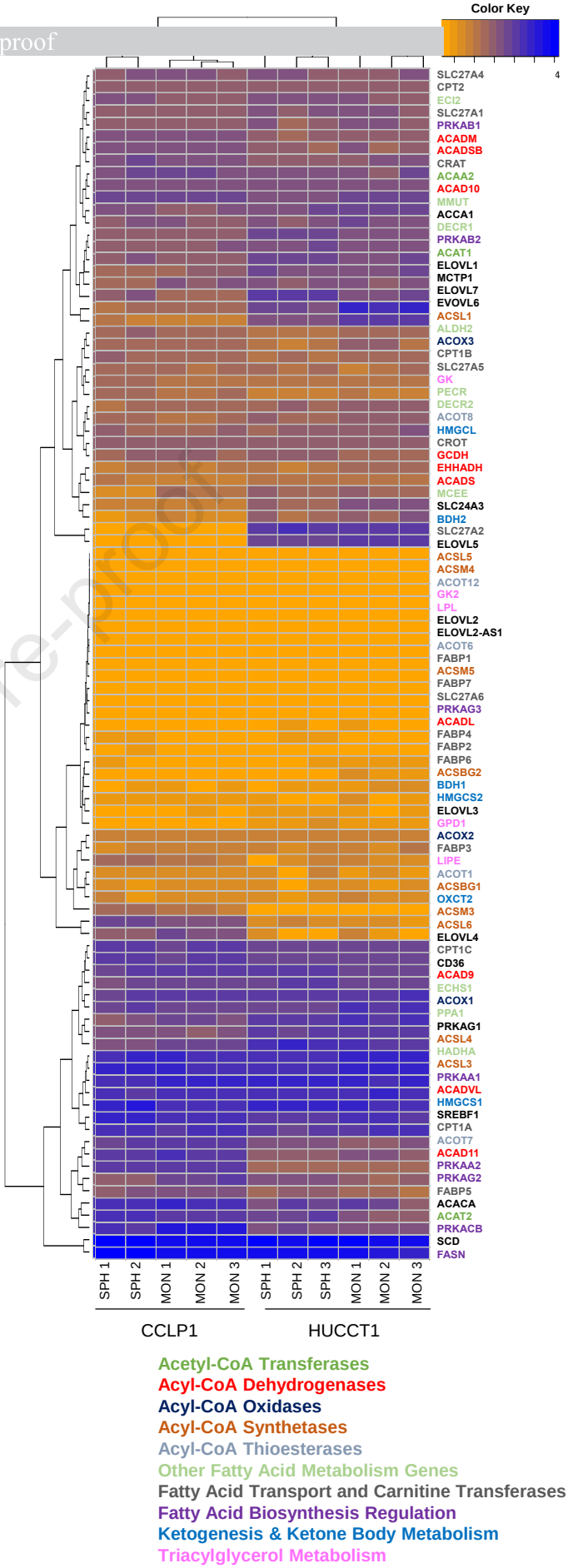

C

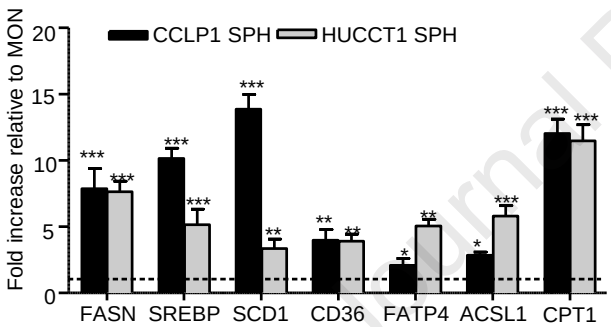

D

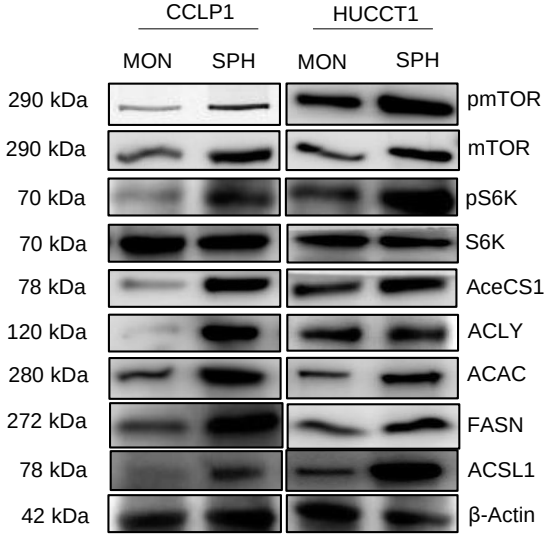

Figure 4

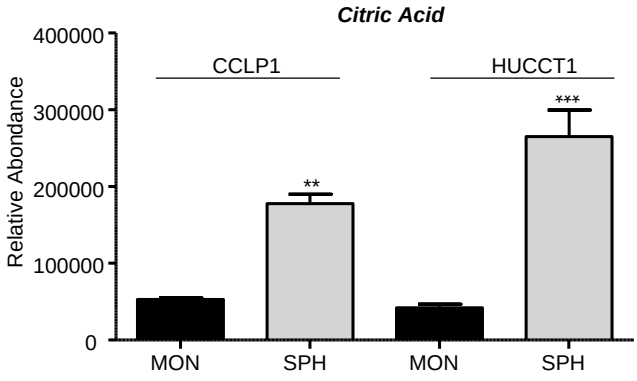

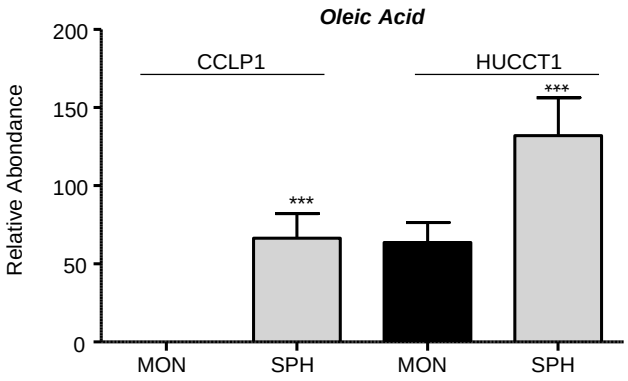

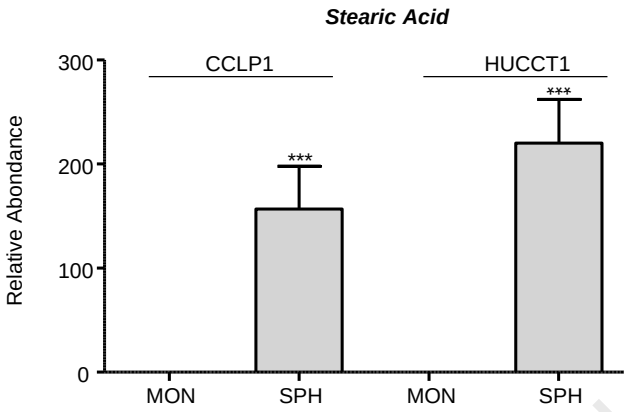

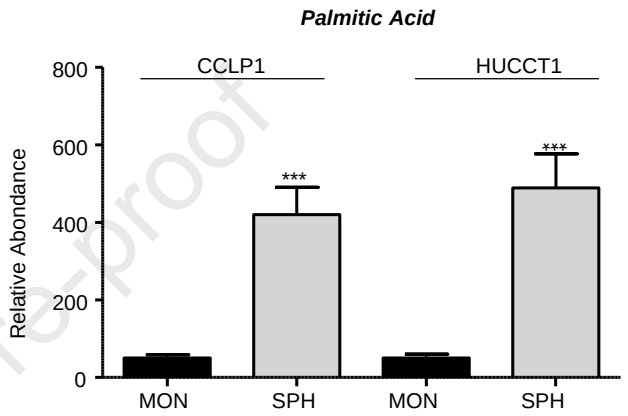

Figure 5

A

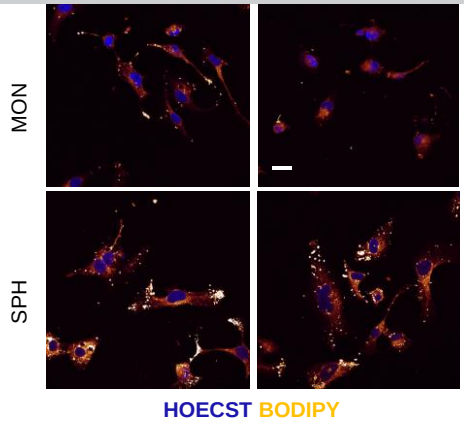

B

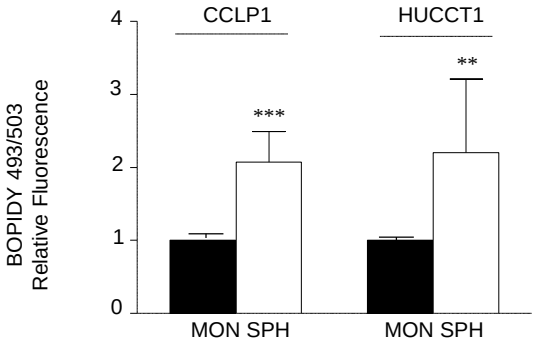

C

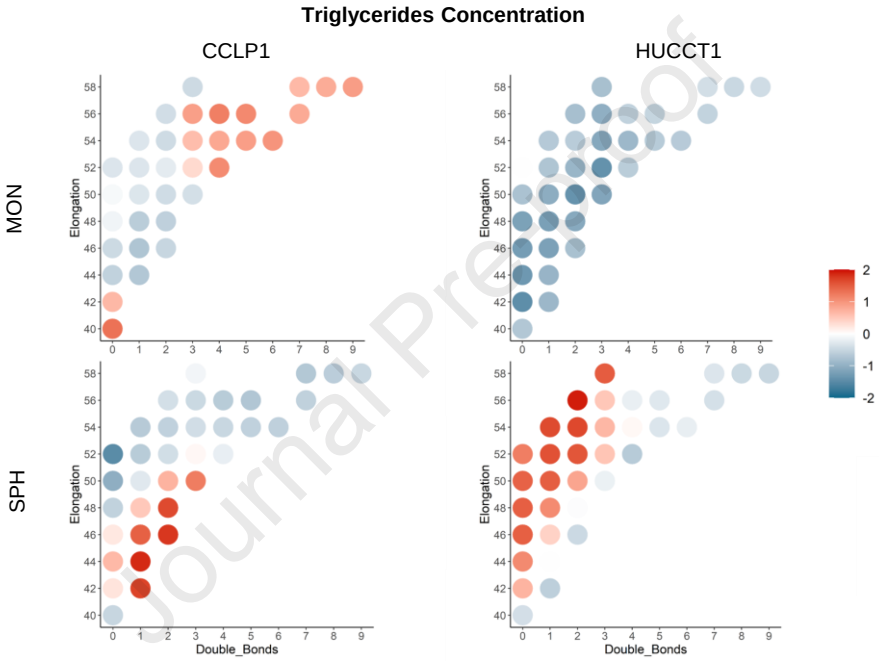

D

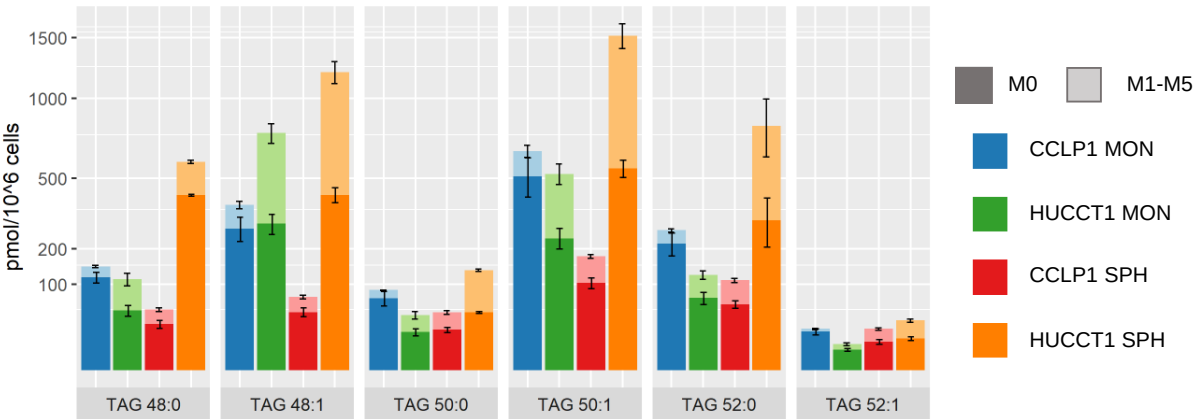

	% de novo synthesized TG *p<0.05 MON vs SPH					
	TAG 48:0	TAG 48:1	TAG 50:0	TAG 50:1	TAG 52:0	TAG 52:1
CCLP1 MON	20%*	27%*	20%*	21%*	13%*	19%*
CCLP1 SPH	56%	62%	51%	55%	38%	42%
HUCCT1 MON	43%*	37%*	52%*	41%*	53%*	47%*
HUCCT1 SPH	67%	65%	67%	63%	59%	62%

Figure 6

A

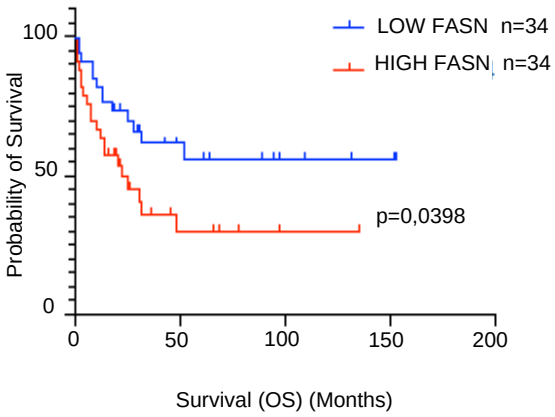

B

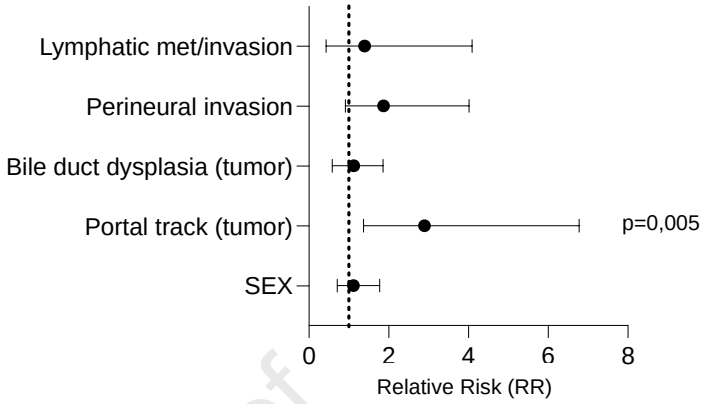

C

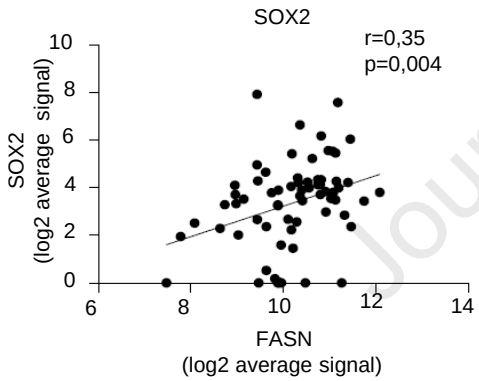

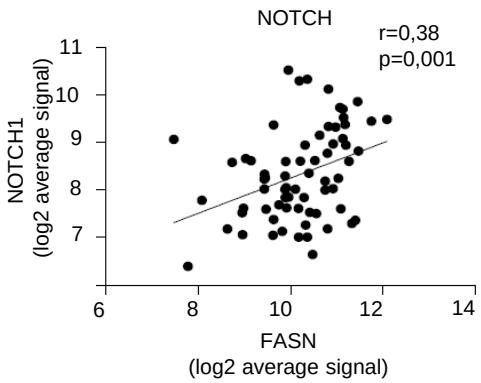

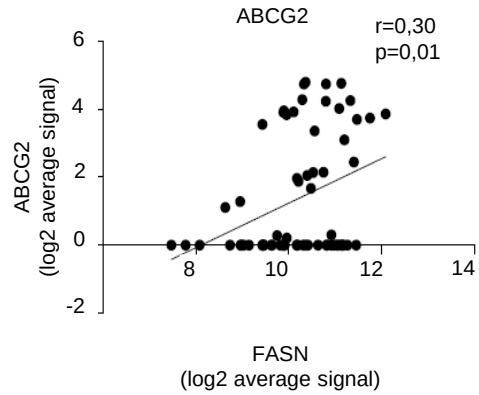

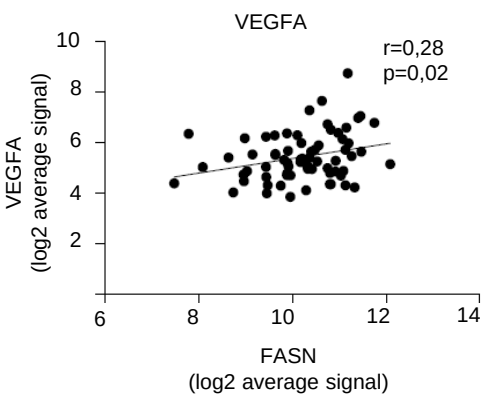

Figure 7

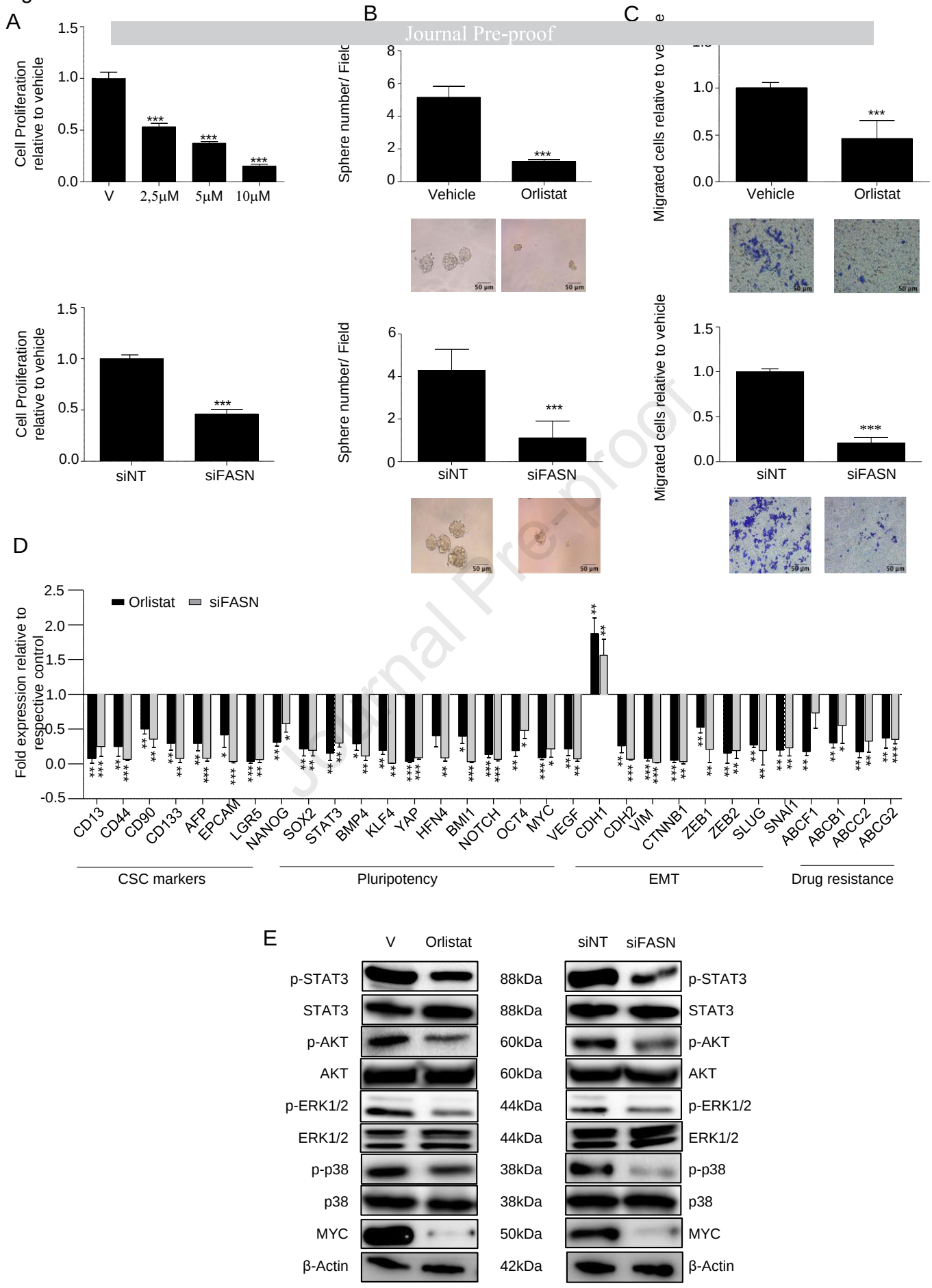
A
B
C
Journal Pre-proof
Cell Proliferation relative to vehicle
1.5
1.0
0.5
0.0
***
V
2,5μM
5μM
10μM
Sphere number/ Field
8
6
4
2
0
Vehicle
Orlistat
Migrated cells relative to vehicle
siNT
siFASN
50 μm
D
Orlistat
siFASN
Fold expression relative to respective control
2.5
2.0
1.5
1.0
0.5
0.0
-0.5
CD13
CD44
CD90
CD133
AFP
EPCAM
LGR5
NANOG
SOX2
STAT3
BMP4
KLF4
YAP
HFN4
BMI1
NOTCH
OCT4
MYC
VEGF
CDH1
CDH2
VIM
CTNNB1
ZEB1
ZEB2
SLUG
SNAI1
ABCF1
ABCB1
ABCC2
ABCG2
CSC markers
Pluripotency
EMT
Drug resistance
E
V
Orlistat
siNT
siFASN
p-STAT3
STAT3
p-AKT
AKT
p-ERK1/2
ERK1/2
p-p38
p38
MYC
β-Actin
88kDa
88kDa
60kDa
60kDa
44kDa
44kDa
38kDa
38kDa
50kDa
42kDa

Figure 8

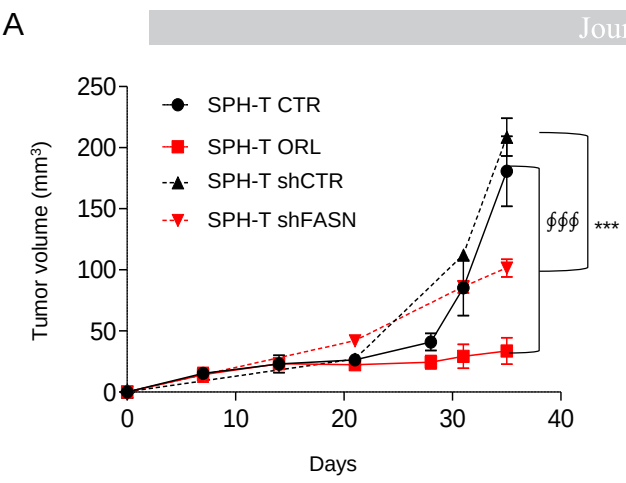

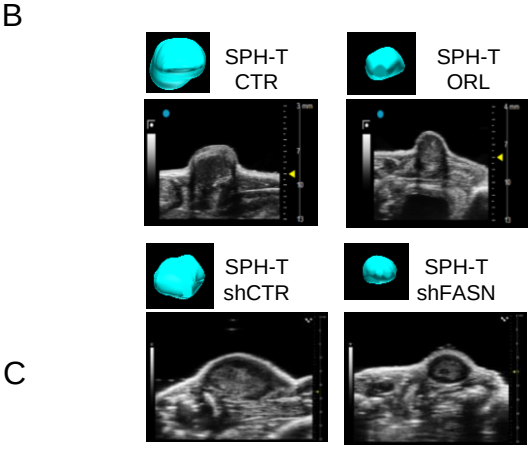

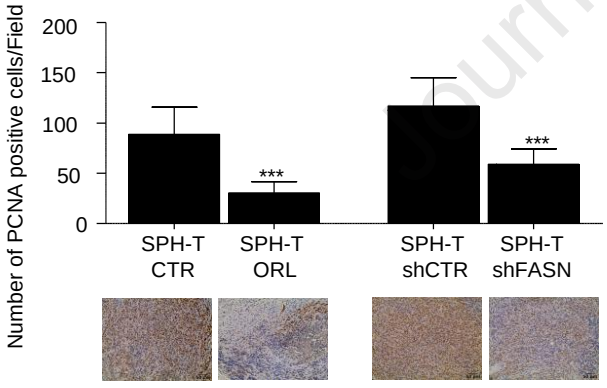

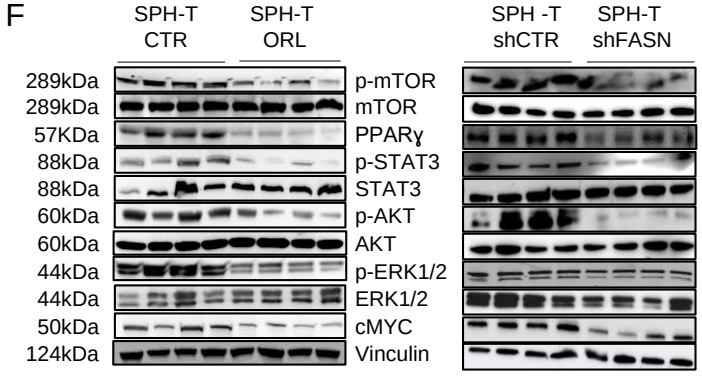

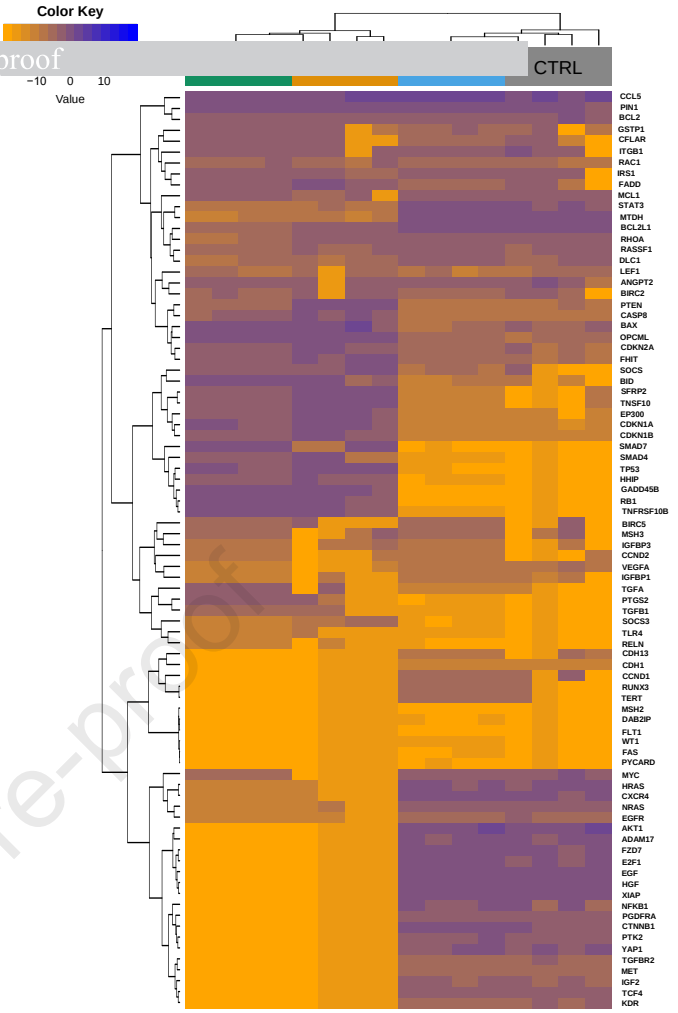

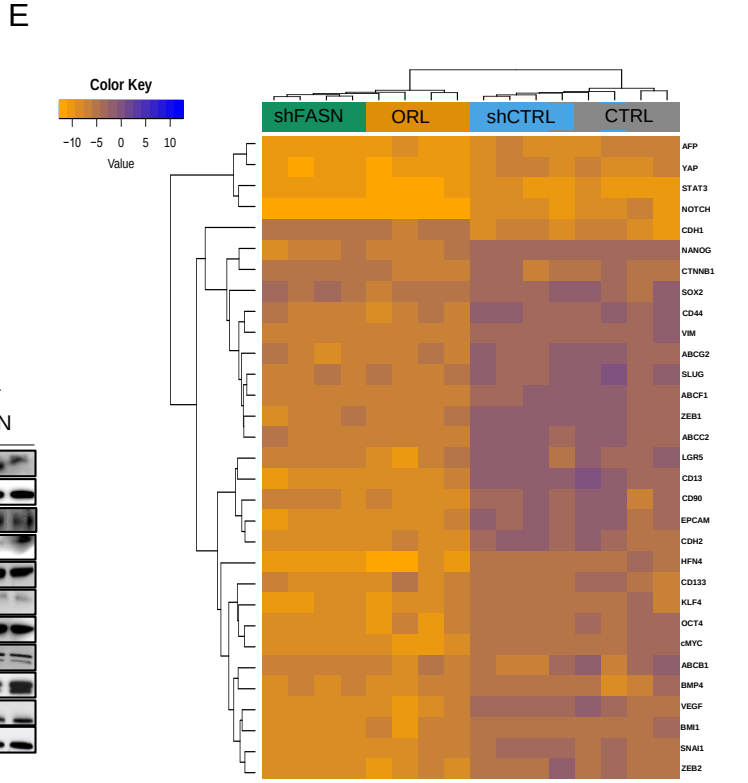

Highlights

- The stem cells in intrahepatic cholangiocarcinoma (iCCA) exhibit disrupted fatty acid metabolism and increased production of specific fatty acids.

- Exposure of iCCA cells to fatty acids results in a notable increase in tumor stem cell program.

- FASN is upregulated in iCCA SPH and its expression correlates with poor prognosis in CCA patients.

- Depletion of FASN or its inhibition reduces the aggressive characteristics of the iCCA cancer stem cell subset